Experimental Investigation of Capillary Blockage of Two Phase Flow in Layered Porous Media

J. D. Shosa
Geology Department
Colby College
Waterville, Maine 04901
email: jdshosa@colby.edu

L. M. Cathles
Department of Earth and Atmospheric Sciences
Cornell University
Ithaca, New York 14853
email: cathles@geology.cornell.edu

Abstract

The flow of two fluid phases through a tube filled with layers of sediments of contrasting grain size has been investigated in the laboratory. The gas phase is introduced uniformly into the sediment pore spaces by decompressing CO_2-charged water flowing through the tube. After a brief transition, the flow of both phases is blocked until the pressure across the tube exceeds a threshold equal to the sum of smaller thresholds at each fine layer. The permeability of the fine layers to the flow of both fluid phases is effectively reduced by at least seven orders of magnitude. Capillary forces are responsible for this blockage. The threshold pressure is predicted by Laplace's capillary formula and the temperature dependence of the threshold pressure is that of interfacial tension. The capillary barriers are highly resistive to permanent rupture by faulting or fracturing.

Introduction

Two-phase flow through layered sediments of low permeability is a subject that has only recently begun to receive much attention (*e.g.*, Celia *et al.*, 1995; Huang *et al.*, 1995; Chaouche *et al.*, 1994; Van Duijn *et al.*, 1995; Borresen and Graue, 1997). Theoretical and experimental attention has mainly focused on homogeneous, isotropic porous media, and the emphasis has been on sediments that are permeable enough to allow production of water or hydrocarbons. Low permeability layered sediments are, however, common in sedimentary basins that are commonly overpressured (*e.g.*, have fluid pressures in excess of hydrostatic) and pressure compartmented. Two-phase flow in these sediments is critically important to understanding overpressuring and pressure compartmentation.

We present experimental evidence in this paper that capillary effects can render *layered* sediments impermeable if a non-aqueous fluid phase is introduced. The capillary sealing requires only grain size contrast and the presence of wetting and non-wetting fluid phases. Since both are difficult to change in nature, capillary sealing, unlike sealing by cementation, porosity reduction, or lithologic barriers, is comparatively invulnerable to permanent rupture by fracturing or faulting. The extensive faulting and fracturing in basins makes capillary sealing an attractive way to explain the fluid overpressuring in sediments and the pressure compartmentation observed in them.

Capillary sealing is not a novel concept. It has been applied to single layers by soil scientists studying the lateral diversion of downward percolating water in the unsaturated zone above the water table (*e.g.*, Miyazaki, 1988; Ross, 1990; Kung, 1990a, b; Steenhuis *et al.,* 1990; Steenhuis and Parlange, 1991). It is familiar to petroleum geologists because capillary seals trap hydrocarbons in basins (*e.g.*, Berg, 1975; Schowalter, 1979). Capillary blockage has been incorporated in models of two-phase

flow in homogeneous, isotropic media where it can be important in controlling fingering (*e.g.*, Lenormand *et al.,* 1988).

Capillary sealing has not been seen as a means of rendering large volumes of sediment impermeable, perhaps because the focus has been on the relatively large scale trapping of hydrocarbons or the ponding of water at a single interface. Hydrocarbons trapped at an interface, for example, block the vertical flow of underlying pore waters, but pore waters are free to move through the interface down dip of the ponded hydrocarbons where they come into direct contact with it. Similarly air in the vadose zone of soils will be free to move around water lenses perched at the base of fine layers. Compartments with different levels of overpressure (in all phases) will not develop in these circumstances. The system will remain permeable on a large scale, even though flow within it may be diverted or ponded locally by capillary barriers. Scaled up capillary seals of this type do not provide a natural way to pressure compartmentalize a large basin.

In finely layered sediments, gravitational segregation could be much less significant than in coarser sections. It is observed to be so at the small scale that the experiments described in this paper find application. The experiments we report here show that the permeability of a grain-size layered porous media with respect to both fluid phases (oil and water) easily can be reduced by over seven orders of magnitude, simply by introducing a non-wetting phase. The experiments show that the capillary barriers at each interface are additive in their blockage of flow. Hence, basin seals could be constructed from an appropriate number of "packages" of gas-filled, fine-coarse sediment layers. The seals that develop would block the flow of all fluid phases and be invulnerable to fracturing and faulting.

Our experiments illustrate how capillary seals could operate in basins. We first discuss experiments and then discuss their application to layered sediments in basins. The experiments do not resolve all the questions that can be raised, but answer some questions and clarify others that need to be resolved by further work.

Experimental Investigation of Two-Phase Flow in Layered Porous Media

General Experimental Design and Procedure

Our experiments were performed in the flow-through system shown in Figure 1. The system consists of an HPLC pump that delivers steady flow through a 0.5 m long stainless steel, sediment-packed sample tube (I.D. 12.7 mm). A backpressure regulator allows flow through the system only when an imposed backpressure is exceeded. Experiments were run on sample tubes packed with 2, 5, and 8 sediment "packages." The packages consisted of a ~11 mm layer of industrially ground quartz having a grain diameter of 45-μm (coarse silt size), a 13 to 15 mm layer of fine-ground industrial quartz having a grain diameter 2-μm (very fine silt to clay size), and a ~11 mm coarse layer identical to the first. The remaining volume of the tubes was filled with quartz particles of 0.5mm diameter (coarse sand). Only the 2-μm layer is critical in the experiments. The 45-μm particles served to hold the fine particles in place. A tube with five 2 μm layers is drawn to scale in Figure 2.

To assure that there was no air in the sediment-filled tube, the tube was filled with dry sediment and the system plumbing was flushed with CO_2 gas so that all the pore space air was replaced by CO_2. The entire system was then evacuated and saturated with water. This procedure, and the high solubility of CO_2 in water, assured that there was no gas in the sediment pores at the start of each experiment. This was found to be critical for accurate single-phase measurements. Even a little gas in the pore space compromised the single-phase flow results.

Having eliminated all gas from the tube, the system pressure was raised and the water in the tube was displaced by a single-phase aqueous sodium bicarbonate solution. When the system pressure was lowered below the partial pressure of CO_2 of this solution, a separate CO_2 gas phase formed and capillary force between the gas and liquid changed the flow of water and gas in the tube. If the pressure at the discharge end of the tube was reduced to atmospheric, flow under two phase conditions stopped even when a large pressure difference still existed across the tube. This situation contrasts sharply with single-phase flow, where opening the discharge end to the atmosphere under no-flow conditions (piston pump turned off) would quickly produce atmospheric pressures throughout the tube.

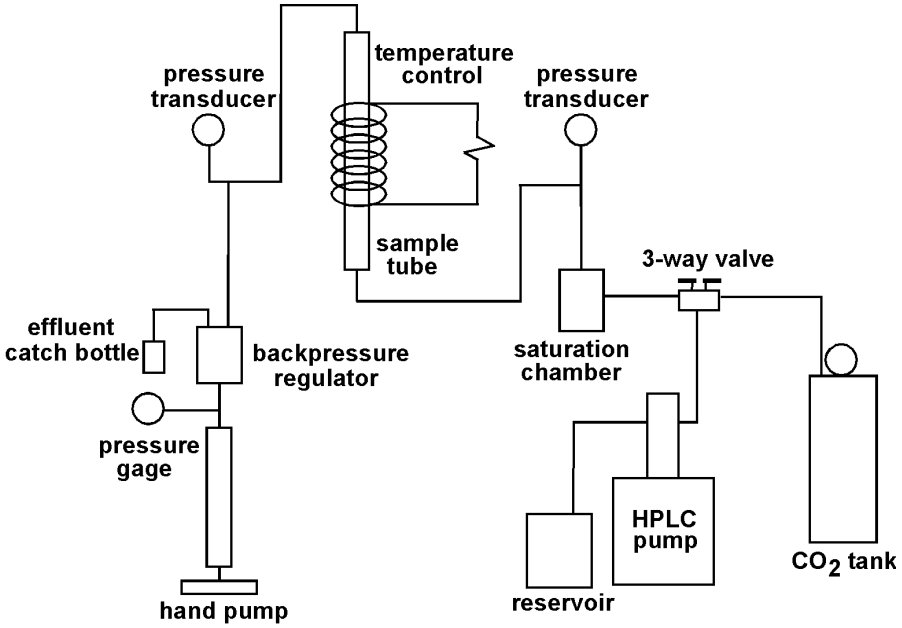

Figure 1. Schematic diagram of the experimental system. A high-pressure liquid chromatography (HPLC) piston pump was used to push one- and two-phase fluids through a ~0.5m long 0.01m I.D. sample tube containing alternating ~15mm thick fine-grained sediment layers in a coarse-grained sediment matrix. Pressure at the exit end was controlled by a backpressure regulator. Tube temperature could be controlled from 20º to >100ºC. Pressure transducers measured pressure at the intake and discharge ends of the sample tube.

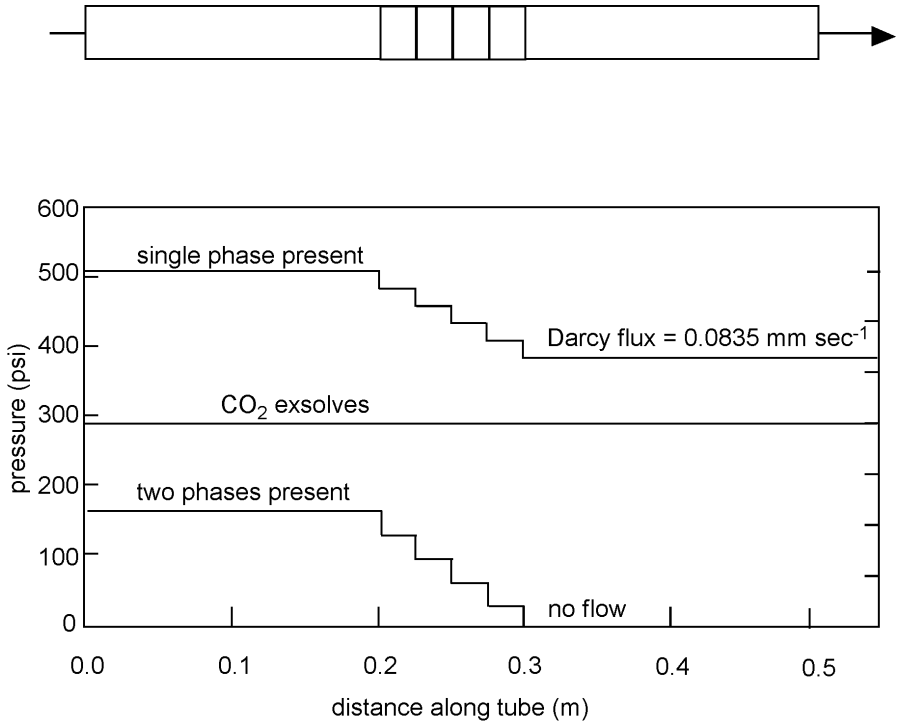

Figure 2. Schematic pressure profiles across the sample tube for the 5-layer experiment. The upper curve shows the pressure profile for a single-phase water flux of 0.0835 mm-sec^{-1}. Pressure at the entry and discharge ends of the tube were measured; the discrete pressure drops at the 2 μm layers are inferred. The middle horizontal line at 190 psi (2.0MPa) is the pressure at which CO_2 exsolved from the fluid. Below this line two fluid phases are present (CO_2 and water). The bottom curve shows the pressure drop under static two-phase conditions.

Figure 2 illustrates our general experimental procedure for the five 2-μm-layer experiment. The top curve shows the pressure profile across the tube for a single-phase flux (Darcy flow rate) of 0.0835 mm sec^{-1}. Pressure drops occur across the low permeability fine layers but are negligible elsewhere. Actually, the pressure drop across the entire tube is measured and equal pressure drops across the fine layers are inferred. The fine horizontal line at 290 psi (2 MPa) shows the pressure at which CO_2 exsolved in the 5-layer experiment. The lower curve shows the static capillary pressure drop across the tube that persists indefinitely after pressure at the discharge end has been reduced to atmospheric. Our procedure was to record the single phase pressure drop across the tube at several flow rates, twice during the experiment: once before the system pressure was reduced and the two-phase measurements made, and again after the two-phase measurements were completed and the system had been re-pressured. We will discuss the single-phase flow measurements first and then the two-phase experiments.

Single-Phase Measurements

The resistance to single-phase flow was measured before and after each two-phase flow experiment. Water was driven through the system at various flow rates and the pressure drop across the tube was measured at each rate. After the two-phase experiments on a particular tube were completed, the system pressure was increased, CO_2 re-dissolved, and the single-phase tests repeated. The results of these "before and after" tests are shown for the 5- and 8-layer experiments in Table 1 and plotted in Figure 3. The black dots show the pressure drops before, and the open circles show the pressure drops after the two-phase flow experiment. All single-phase flow measurements were made at 20ºC.

The single-phase pressure drop across the sediment-filled tube at various flow rates are compared to the drops predicted by Darcy's Law and the Kozeny-Carmen equation (lines in Figure 3). The bulk porosity ϕ of the sediments in the tube was determined by recording the volume of water required to fill the sediment-packed tube. Porosities measured in this fashion ranged from 0.46-0.48 for all experiments. We assume that the porosity is the same for all grain sizes of sediments. This is reasonable since porosity does not depend on grain size and the loading procedures were the same for all layers. A reasonable estimate of porosity is adequate here as our intention is only to show that the measured pressure drops are reasonable for single-phase flow and thus establish a context for interpreting the two-phase capillary effects, not to make accurate measurement of the sediment permeability.

Table 1. Single-phase pressure drops measured across the tube at various flow rates before and after the two-phase experiments.

V_w [mm-sec-1]	Pressure drop across tube before two-phase experiment [psi]	Pressure drop across tube after two-phase experiment [psi]
	5-Layer Experiment	
0.0167	34.35	30.57
0.0334	57.02	55.13
0.0500	77.80	75.91
0.0668	100.47	104.25
0.0835	115.59	121.26
	8-Layer Experiment	
0.167×10^{-3}	7.79	7.83
0.334×10^{-3}	11.68	
0.500×10^{-3}	15.46	11.58
0.668×10^{-3}	21.12	
0.835×10^{-3}	24.90	22.92

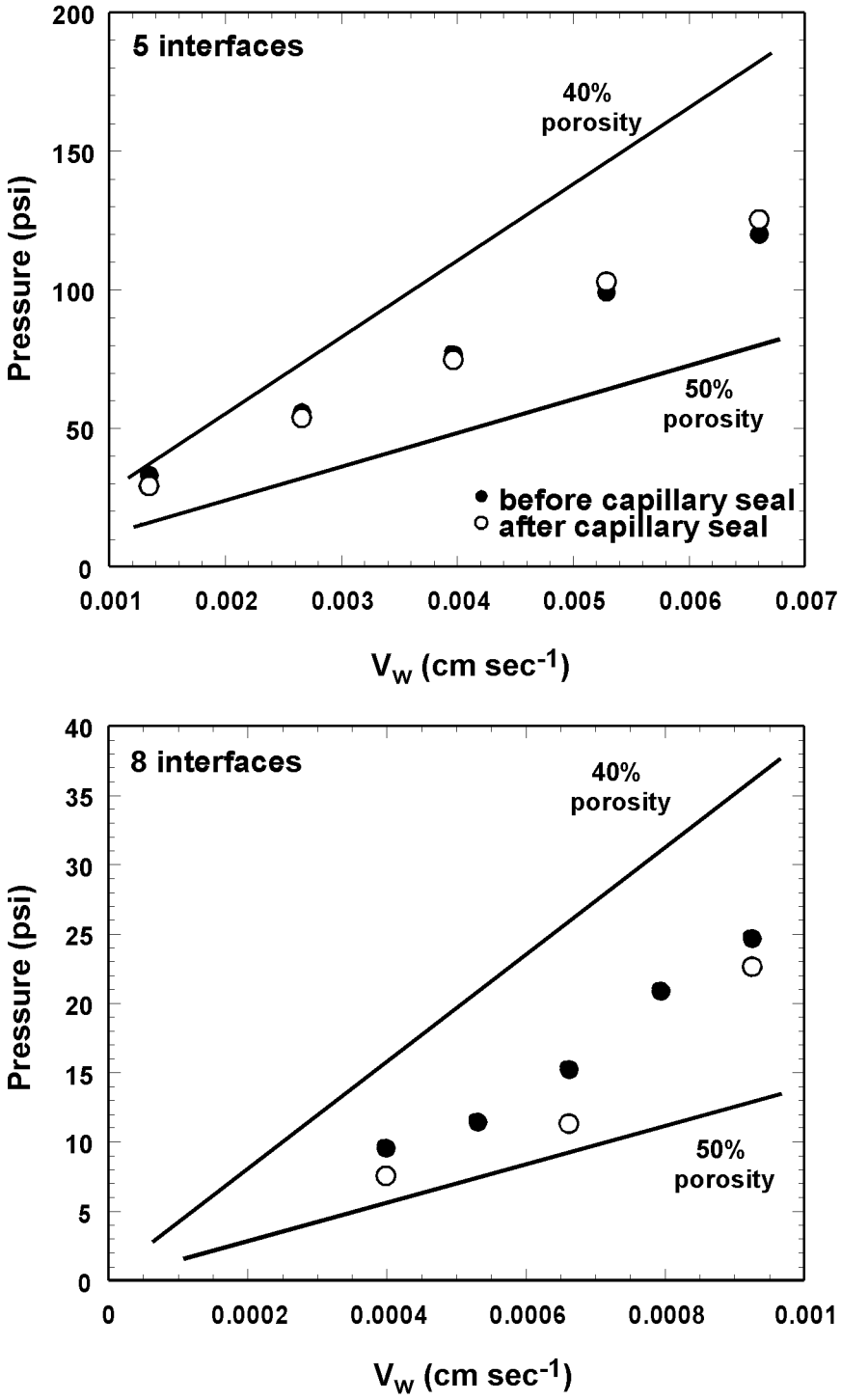

Figure 3. Pressure drop across tube under single-phase conditions before and after the two-phase experiments as a function of flow rate for sample tubes with five and eight 2 μm layers. The solid lines show the pressure drops predicted as a function of low rate using equations (2) and (3) in the text. The porosity of all sediments in the tube was between 46 and 48%. Predictions for this porosity range would overlie the measurements.

The permeabilities, k_i, of the sediment layers with grain diameters d_i were calculated using the Kozeny-Carmen relationship shown below (Equation 1; Bear, 1972; Freeze and Cherry, 1979) for porosities of 40 and 50% with the results shown in Table 2.

$$k_i = \frac{d_i^2}{180}\frac{\phi^3}{(1-\phi)^2} \tag{1}$$

In this equation d_i is the grain diameter of layer i, and ϕ is the porosity of the layer, which we assume equals the bulk porosity of all sediments in the tube. The pressure drop across each sediment layer was then summed to obtain the total pressure drop the tube at various flow rates (Equation 2):

$$\Delta P = V_w \mu_w \sum_{i=1}^{n} \frac{h_i}{k_i} \tag{2}$$

where,

ΔP is the total pressure drop across the tube;

V_w is the Darcy flux of water through the tube;

μ_w is the dynamic viscosity of water at 20ºC, and

k_i is the intrinsic permeability of the i^{th} sediment layer having a thickness h_i.

The resulting calculated pressure drops are shown as solid lines in Figure 3. As ahown in Figure 3 the pressure drops predicted for the measured bulk porosity of 46 to 48% will virtually overlie the pressure drops measured in the single-phase flow tests. This agreement shows:

1. we can predict the resistance to single phase flow in the sediment tube using established equations, measured grain sizes and porosities (which is not remarkable);
2. that the permeabilities of the layers remained unchanged after each multiphase experiment; and
3. that all gas affecting flow could be re-dissolved when the system was re-pressured.

Table2. Calculated permeabilities (k_i) of the sediments used in the experiments for porosities of 40 and 50%, based on equation (2).

Grain Diameter [μm]	Permeability [m^2] at 40% porosity	Permeability [m^2] at 50% porosity
2	3.95×10^{-15}	1.11×10^{-14}
45	1.90×10^{-12}	5.60×10^{-12}
500	2.47×10^{-10}	6.95×10^{-10}

Measuring Capillary Barriers under Static (no flow) Conditions.

After the first set of single-phase measurements was completed, the HPLC pump was turned off. Pressure at the discharge end was slowly reduced by reducing pressure on the backpressure regulator in small increments over a period of ~5 hours as shown in Figure 4. Pressures at both ends of the tube were similar during this procedure until gas exsolved as a separate phase. When pressure was sufficiently reduced that a gas phase was present within the pores of the sediment, we observed that the pressure at the exit end of the tube fluctuated for about a half-hour. During this time interval (crosshatched band in Figure 4) both fluid phases were mobile in the tube. The backpressure regulator was adjusted to atmospheric and the exit pressure stabilized at atmospheric an hour or so after gas first exsolved. It was observed that the pressure at the entry end of the tube stabilized at a pressure lower than the pressure at which CO_2 first exsolved. Thereafter a stable pressure drop remained across the tube and there was no detectable flow of either gas or water through the tube for as long as we chose to monitor the system.

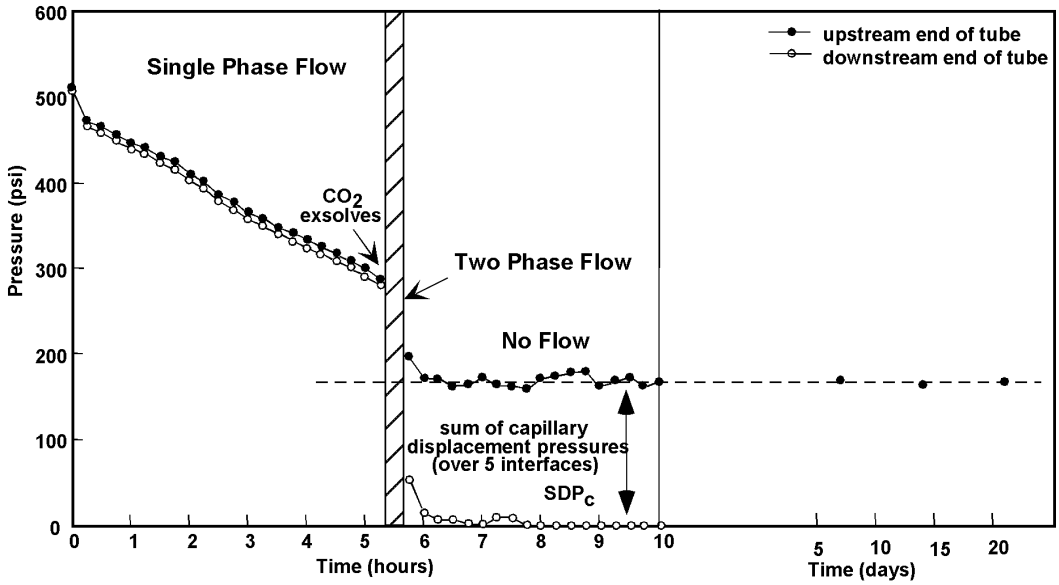

Figure 4. Plot of pressure at the upstream (solid balls) and downstream (open circles) ends of the sample tube as pressure at the discharge end is slowly reduced to atmospheric for the 5-layer experiment. Within the crosshatched vertical there was two-phase flow in the tube. Before this flow was single phase. After this capillary seals were established and the pressure jump for each was at the pressure threshold; there was no flow of either phase through the tube.

Figure 4 illustrates the pressure changes that occurred across the tube as backpressure was reduced during the experiment in which the tube contained five 2 μm layers. In this five-layer experiment, a stable pressure drop across the tube of 163 psi (1.12 MPa) remained unchanged for three weeks with the discharge end of the tube open to the atmosphere. We measured the pressure drops for the two, five, and eight 2-μm layers in the tube in the fashion described above and determined the capillary pressure drop per fine-coarse package by dividing by the number of packages.

In each experiment (*e.g.*, for each tube with different numbers of 2 μm layers) we also measured the temperature-dependence of the stable capillary pressure drops. To accomplish this, the tube was wrapped with heating wire in such a way that there was a constant temperature along and within the parts of the tube that contained the 2-μm layers. After completion of the 20°C experiment, the tube was heated first to 50°C, then 75°C, and finally to 100°C. In each case it took a few hours for the pressure to stabilize after the temperature had been reset. When the pressures stabilized, the total pressure drop across the tube was measured (Table 3). The stable, no-flow pressure drops measured at various temperatures in the 5- and 8-layer experiments were plotted as a function of temperature (using black squares and dots) in Figure 5. The pressure drops per interface under no flow conditions shown in Figure 5 are larger than the pressure drops at the greatest flow rates of the single-phase experiments (Table 1).

Interpretation of the Static, Two-Phase Experiments

The simplest explanation of the results shown in Figure 5 is that capillary forces are blocking the flow of both fluids at each 2-µm layer. If there is no pressure gradient imposed across the tube, capillary suction will pull water into the fine layers and expel any gas that may have exsolved there, so the fine layer becomes saturated only with water and contains no mobile gas. If a pressure gradient is imposed across the tube, this will occur, but at the same time, as water leaks through the fine barriers, gas will accumulate on the high-pressure side of each 2-µm layer. If it eventually blocks all the pores to fluid entry, the flow of both fluid phases will be stopped, and the static pressure drop across each fine layer will equal the capillary gas entry pressure, ΔP_c (Equation 3; Berg, 1975; Kung, 1990; Steenhuis *et al.*, 1990, 1991):

$$\Delta P_c = 2\sigma\left(\frac{1}{r_{fine}} - \frac{1}{r_{coarse}}\right) \quad (3).$$

Table 3. Measured two-phase static pressure drops as a function of temperature.

Temperature [ºC]	Static two-phase pressure drop [psi] across tube	Static two-phase pressure drop [psi] per 2-μm layer
	5-layer experiment	
20	162.78	32.56
50	155.77	31.15
75	145.87	29.16
100	135.48	26.90
	8-layer experiment	
20	285.62	35.70
50	276.18	34.52
75	257.28	32.16
100	228.95	28.62

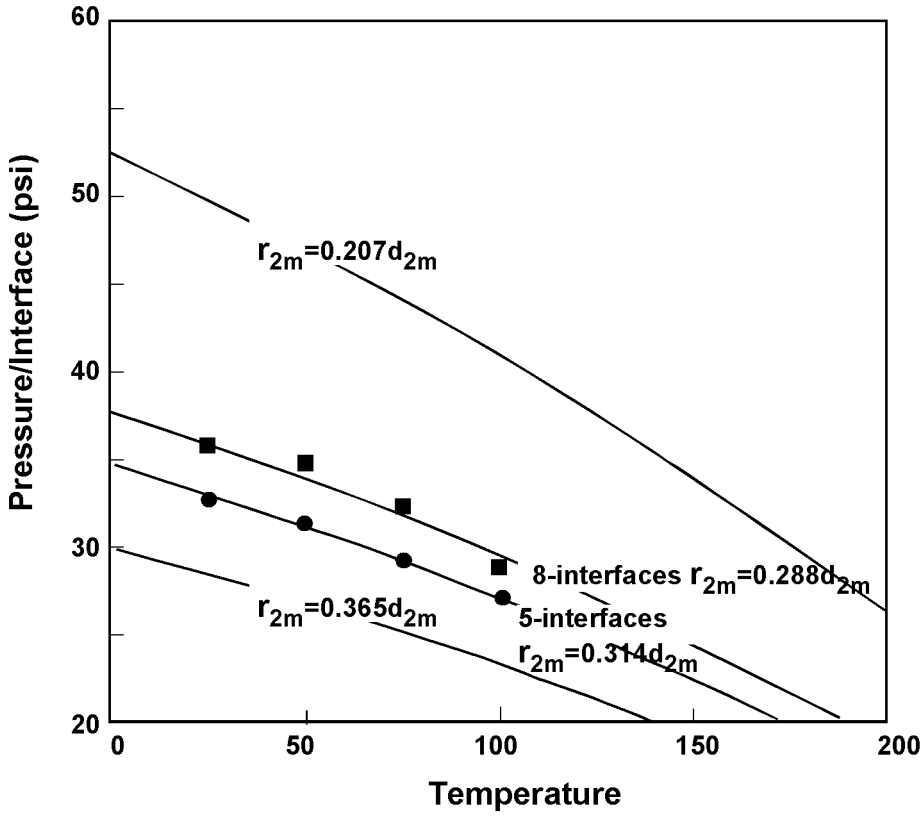

Figure 5. Static (no flow) pressure drop per 2-μm layer in the 8- and 5-layer two-phase experiments measured at different temperatures are shown in square and diamond symbols respectively. The solid lines show the pressure drops predicted by equation (1) for two estimates of pore throat size. The outer pair of lines uses the maximum and minimum pore throat size for cubic-packed 2μm beads. The inner pair of lines estimates the pore throat size of the 2μm layers using equation (5) and a porosity of 46-48%. The temperature-dependence of the curves derives from temperature dependence of interfacial tension between CO_2 and water.

In Equation 3, ΔP_c is the pressure change across the interface required to induce the entry of CO_2 into water saturated 2-μm layers. The subscript c indicates that it is a capillary pressure difference deriving from work against capillary forces, σ is the temperature-dependent interfacial tension between CO_2 gas and water, r_{fine} is the maximum pore throat radius of the 2-μm layer, and r_{coarse} the smallest pore throat radius of the adjacent coarse layer. Equation (3) is an adaptation of Laplace's Law to the boundary of porous media of different grain size with the contact angle taken to be zero.

The lines in Figure 5 show the capillary pressure drops across a 2-μm layer adjacent to a 45-μm layer calculated as a function of temperature using (Equation 3) and the temperature-dependent interfacial tension between CO_2 and water. Water-CO_2 interfacial tension decreases approximately linearly by 18% from 0.073 N/m at 20ºC to 0.060 N/m at 100ºC (Washburn *et al.,* 1928). The outer and inner pairs of lines are based on two different estimates of the maximum and minimum pore throat size, $r_{2\mu}$, in the 2μm layers. The outer pair of curves in Figure 5 is calculated assuming the sediment grains are packed cubically. This is justified somewhat by the fact that the measured bulk porosity of the sediments (46-48%) coincides with the theoretical porosity of cubic packing (48%). For cubic packing the range of pore throat size is $0.207d_{2\mu}$ to $0.365d_{2\mu}$ (Graton and Fraser, 1935), where $d_{2\mu}$ = 2-μm. The effective pore throat radii for the 2μm sediment also was estimated using an expression derived in Revil *et al.* (1997):

$$r_{2\mu} = \frac{2}{3}\frac{d_{2\mu}}{(\phi - \phi_p)^{-m} - 1} \tag{4}$$

In Equation 4, $r_{2\mu}$ is the effective pore radius of the 2-μm layer, $d_{2\mu}$ the average diameter grains in the layer, ϕ the porosity, ϕ_p the "percolation porosity", and m is Archie's electrical conductivity exponent. Since, for perfectly spherical grains, m = 3/2 (Sen *et al.*, 1998) and ϕ_p lies between 0.02 and 0.03 (Revil and Cathles, 1999), (Equation 4) gives an effective pore throat radius of the 2-μm layer of between $0.262d_{2\mu}$ and 0.302 $d_{2\mu}$, for porosities between 46 and 48%. This narrower range of effective pore-throat radii brackets the measured pressure drops across each 2-μm layer for all temperatures (Figure 5). Equations (3) and (4) are clearly able to accurately predict both the static pressure drop across each 2-μm layer and its temperature dependence with considerable accuracy, and this success indicates the blockage is capillary in nature.

Capillary Barriers Under Flowing Conditions

The capillary barriers behave according to (Equation 3) under no flow conditions, but how will they function when fluid is forced through them? Will they re-heal and remain effective after significant amounts of water and gas have been driven through? Will the independence of the 2-μm layers be compromised by fluid throughput? To address these questions we drove significant two-phase flow through a tube containing two sediment packages after CO_2 had exsolved and the capillary barriers had formed. The experiment temperature was 20ºC. For a single-phase flow rate of 1.67 mm^3 sec^{-1} the pressure drop was determined to be 10.44 psi (0.072 MPa), close to the predicted 9.64 psi (0.066 MPa). When the system pressure was lowered so that a gas phase exsolved from the pore fluid, the pressure required to drive flow at the same rate increased by a factor of 7 to 73.1 psi (0.50 MPa). Assuming that the capillary pressure drop is in addition to the viscous flow resistance and that the gas channels occupy a small percentage of the 2-μm layer as would be expected by the low viscosity of gas relative to water, the capillary barrier will sustain approximately 73.1-10.44 = 62.1 psi, a value close to that expected for two capillary barriers of 68.2 psi (0.47 MPa). See Figure 7 and discussion in next section.

Injection (pumping) was continued until about 10^4 mm^3 of CO_2-charged water had been driven through the tube. The injected fluid volume represents about 37% of the total pore volume in the tube, 122% of the pore volume of the tube from the entry end to the first 2-μm layer, and about 12 times the pore volume of each 2-μm layer. No change in the pressure drop across the tube was observed during

this time, indicating that neither of the two barriers was compromised by this amount of two-phase throughput. The experiment suggests that capillary pressure drops at fine layers will be maintained even after substantial volumes of gas or gas-saturated water have been forced through the capillary barriers.

Cumulative Response of the 2-μm Capillary Barriers

Figure 6 shows that the total pressure drop across the tube increases linearly with the number of 2-μm layers. The flow blockage by individual fine layers is thus cumulative. This aspect is crucial to the operation of capillary seals in basins. The best estimate of the capillary pressure drops per 2-μm layer at 20ºC for all experiments is 34.1 psi (0.235 MPa), as indicated by the top curve in Figure 6.

Further Deductions from the Two-Phase Experiments

The pressure recorded by the upstream pressure gauge when CO_2 first exsolves measures the concentration of CO_2 in the single-phase fluid. The pressure recorded by the upstream gauge when two-phase flow has been stopped by the capillary barriers measures the concentration of CO_2 in solution under static, no-flow conditions. The difference gives the CO_2 exsolved from the fluid from the front of the flow tube to the first 2-μm layer (which we shall refer to as the first compartment). We can compute the volume of this exsolved CO_2 from the density of CO_2 at the appropriate pressure and temperature. For example, Figure 4 shows CO_2 exsolves at 290 psi (2MPa) in the 5-layer static experiment. Thus, for a Henry's law constant of 0.0339 moles/MPa-liter (Stumm and Morgan, 1996, p.214), the dissolved CO_2 is 0.678 moles/liter. Flow ceased at a pressure of 163 psi (1.12MPa), at this pressure the dissolved CO_2 concentration is 0.380 moles/liter. Thus 0.28 moles of CO_2/liter had exsolved as a separate gas phase when flow stopped. The density of CO_2 at 163 psi is 0.547 moles/liter (calculated using the Behar *et al.*, (1985; 1986) equation of state). The volumetric gas saturation (m^3gas/m^3 water) in the first compartment when flow stops is thus 0.28/0.547 = 0.54. This assumes that gas and water leaked through the first -μm layer in approximately equal volumes in the transition period before flow stopped. When static conditions were established, the pores in the first compartment thus contained about equal volumes of CO_2 gas and water.

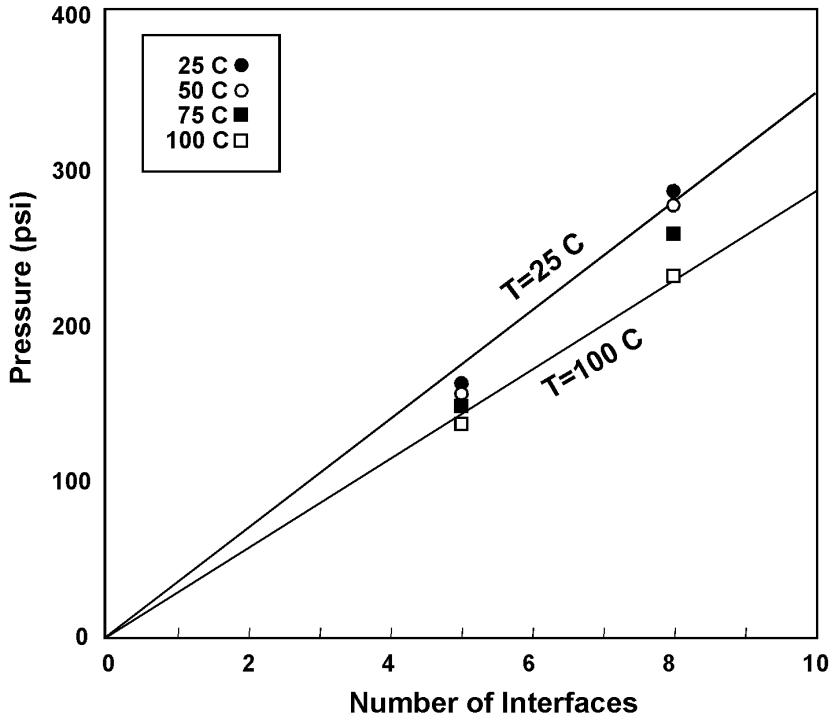

Figure 6. Static (no flow) total pressure drop across sample tube at various temperatures plotted as a function of the number of 2 μm layers in the tube. Solid lines show the pressure drops predicted by equation (1) for a pore throat radius of 0.059 μm and 20º and 100ºC.

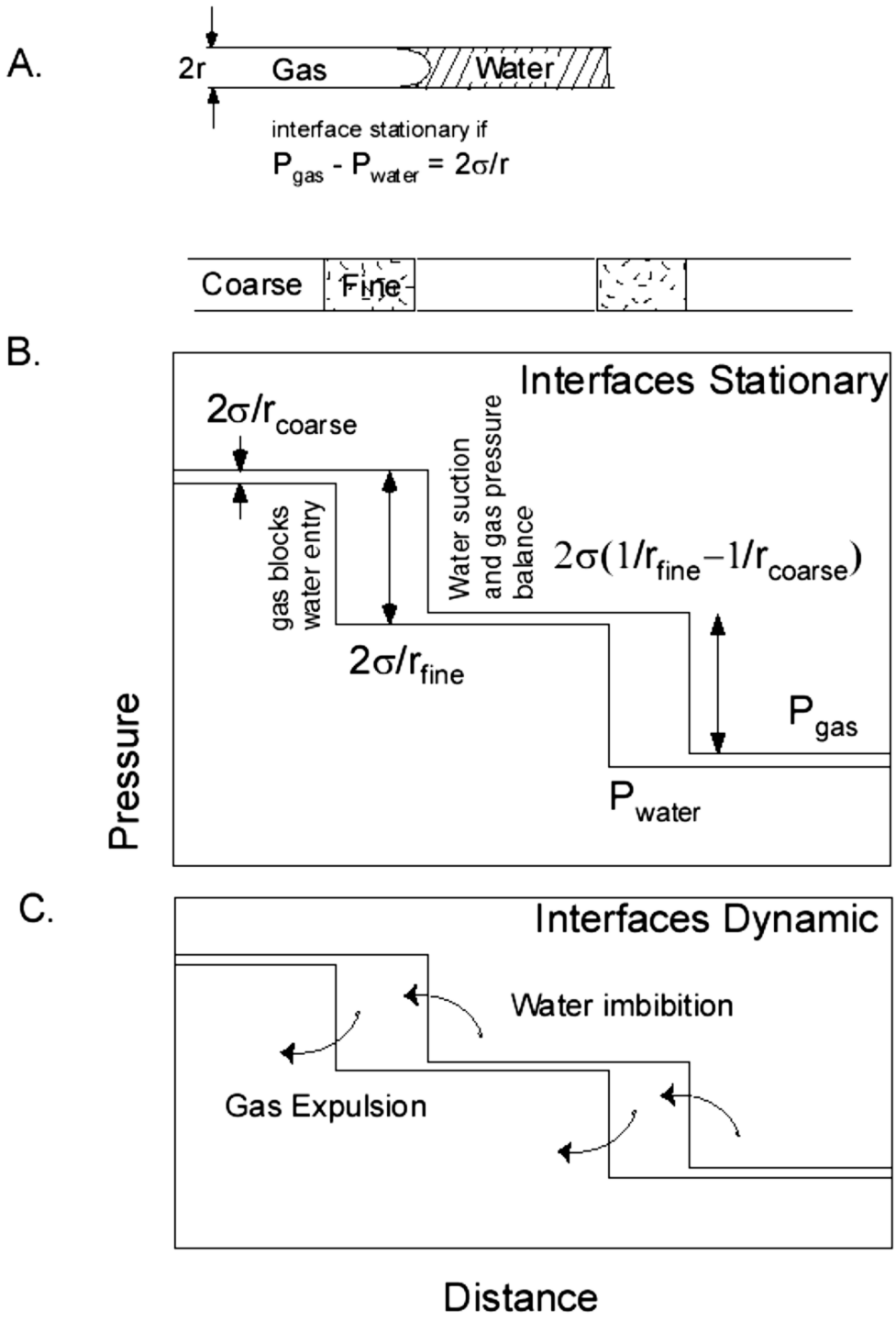

Figure 7. A. Illustrates the pressure conditions in the gas and water phases that must pertain if an interface between gas and water is to be stationary. B. Applies this condition to alternating fine and coarse layers. Gas-blocks the entry of water into the fine layer on the high-pressure side of the fine layers; water suction is balanced by gas pressure on the low-pressure side. Equation (1) is a natural consequence of the stationary interface criteria. C. If pressure is reduced across the system, water will be drawn into the fine layer by capillary forces and gas will be expelled. If pressure across the system is increased both water and gas will flow through the fine layers. Considering perturbations from (B), water will flow through the system only when the pressure gradient exceeds the static level shown in (B).

The protracted pressure maintenance shown in Figure 4 allows us to estimate the maximum effective permeability of the 2-μm layers to water under no flow conditions. The magnitude of the minimum permeability reduction in 2-μm layers is astoundingly large. This large reduction is important both practically and theoretically.

The capillary pressure drops across each 2-μm layer in the 5-layer experiment should be approximately equal. The leakage rates (if any) across each should therefore also be about equal. The compressibility of fluid from the HPLC piston to the first 2-μm layer (the first compartment) is dominated by the 1.5 x 10^{-4} psi^{-1} (0.0218 MPa^{-1}) compressibility of CO_2 at 163 psi (1.12 MPa) and 25°C (Matthews and Russell, 1967, Table G.7a). In 3 weeks time the change in pressure in the first compartment measured by the upstream pressure gauge is less than 5 psi (0.034 MPa). This is a maximum estimate. On average the change is zero, the variability coming from a level of noise in the pressure transducers (see Fig. 4).

A pressure drop of 5 psi would require expulsion of the following fluid volume across the first 2-μm layer (Equation 5):

$$V_{expelled} = \phi S_g c_g \Delta p A L \tag{5}$$

where,

$V_{expelled}$ is the maximum fluid volume expelled from the packed tube and plumbing system between the HPLC pump and the first 2-μm layer (the first compartment);

ϕ is the porosity of the tube filling (0.46);

S_g is the gas saturation in the first compartment (0.5),

c_g is the compressibility of gas at 163 psi (1.12 MPa) and 25°C;

Δp is the maximum pressure change of the first compartment (<5 psi);

A is the cross sectional area of the tube (127 mm^2); and

L is the length of the first compartment (195 mm).

For these parameter values, the maximum fluid volume that could have leaked from the first compartment is 4.3 mm^3. Over three weeks the maximum leakage rate is therefore 1.89 x 10^{-8} mm sec^{-1}, about 6 orders of magnitude less than the 0.016 mm sec^{-1} of the slowest flow rate single phase experiment (Table 1).

We can estimate the maximum effective permeability of the fine layers from the maximum leakage rate (Equation 6):

$$kk_r^w(S_w) = \frac{V_w \mu_w h_i}{(\Delta P)/N} \tag{6}$$

where,

k is the intrinsic permeability of the 2-μm layer;

$k_r^w(S_w)$ is its relative permeability at water saturation S_w;

V_w is the Darcy water flux (1.89 x 10^{-9} m sec^{-1});

μ_w is the viscosity of water at the temperature at which the experiment is run (1 x 10^{-3} kg/m-s at 20°C);

h_i is the thickness of the resistive layer (which we take as the full 14 mm thickness of the 2-μm layer);

ΔP is the pressure drop across the tube (163 psi or 1.12 MPa); and

N is the number of 2-μm layers (5 in this experiment).

For these parameter values, $kk_r^w(S_w)$= 1.2 x 10^{-21} m^2 (1.2 nanodarcies). Because the intrinsic permeability of the 2-μm layer at 47% porosity is ~7.4 x $10^{-15}m^2$ (7.4 millidarcies), if we were to account for the blockage by relative permeability, $k_r^w(S_w) \cong 1.6 \times 10^{-7}$. This is expected since the maximum leakage rate is 6 orders of magnitude less than the flow rates in the single-phase experiments and the pressure drop per interface is an order of magnitude more (34.1 psi per fine layer compared to ~3 psi per fine layer).

Discussion

The ease with which capillary barriers can be produced in the laboratory and the extremely small leakage rate of water through the capillary barriers once they form is surprising. However, the distinction of whether the leakage rate is small or actually zero is an important one, because even slight leakage of water through such barriers could be important over the lengths of time (millions of years) available geologically.

A simple argument suggests to us that the flow is not just very small but actually zero. Figure 7 shows the pressure profiles in the gas and water phases that must exist across two fine layers when some gas has penetrated the fine layers and there is no flow of either phase through the layers. Capillary pressure (the difference between gas and fluid pressure) equals 2σ/r, where r is the grain diameter of sediment. Because r is smaller, capillary pressure is larger in the fine layers than in the coarse. Gas pressure is continuous (and water pressure discontinuous) across the fine-coarse interface at the high-pressure side of the fine layer. Water pressure is continuous (and gas pressure discontinuous) across the fine-coarse interface on the low-pressure side of the fine layer. The water pressure discontinuity at the high-pressure side could be considered to result from gas blockage. The gas pressure discontinuity at the low-pressure side is required to prevent water imbibition.

The interesting point is what happens if the pressure change across the layer is reduced. If the pressure drop is reduced, water will enter the fine layer and gas will be expelled as shown in Figure 7c. At pressures drops less than the stationary, no flow value, the flow of both water and gas will be up-pressure, not down pressure. This suggests to us that the flow of both phases is blocked completely by the capillary barriers until the capillary entry pressure of gas and the exit pressure for water (which are equal in magnitude) is exceeded. At pressures less than this, capillary seals will heal themselves by imbibing water and expelling gas. Capillary seals thus act like pressure release valves. Flow through them is best understood in terms of energy or force balance (Schowalter, 1979). The familiar concept of relative permeability is misleading when considering capillary seals.

We conclude that leakage through capillary seals is either zero or so small that it is effectively zero over even geologically long periods of time. Since the blockage at multiple barriers is additive, layered, gas-filled sediments could form substantial seals.

Sediments are deposited in lozenge-shaped packages of widely variable scale. Individual layers can be millimeters to 10's of meters thick. Faulting introduces additional lateral grain-size variations. The grain size contrast in basins is similar to that in our experiments (2μm to much larger grain sizes). A hundred or so, gas-filled sediment layers at ΔP_c~30 psi (0.2MPa) distributed over a few hundred meters could easily account for the ~2900 psi (20MPa) pressure transition from hydrostatic to near lithostatic pressures that typically occurs in basins at about 3 km sediment depth. A smaller number of fine-coarse layers containing hydrocarbons and water within the overpressured zone could produce the interior seals for pressure compartmentation.

The most critical issue for the operation of capillary seals in basins is the rate at which the hydrocarbon and aqueous fluid phases will segregate gravitationally. For finely interlayered sediments, gravity segregation may occur so slowly that it is not a problem. If hydrocarbon bubbles are lodged and form blockages at the intergranular scale, segregation may not occur at all.

Gas-saturated fluids flowing through leaking seals would exsolve the gas required to re-establish the seal. These implications and others are discussed in more detail in Cathles (2001, this issue). Our experiments have not addressed all the questions that could be raised but have established that capillary

blockage is a possible cause of overpressuring in basins. Although questions remain, the experiments show directly how capillary sealing can occur in basins.

Summary and Conclusions

Our experiments suggest the following macroscopic equations may be useful in describing multiphase fluid flow in porous media (Equations 7a, b):

$$V_i = 0 \qquad \text{if} \qquad \nabla P \le f\Delta P_c \tag{7a}$$

$$V_i = \frac{kk_i(S_i)}{\mu_i}(\nabla P - f\Delta P_c) \qquad \text{if} \qquad \nabla P > f\Delta P_c \tag{7b}$$

where,

the subscript i represents either gas or water,

$k_i(S_i)$ is the relative permeability to phase i as a function of the saturation of phase i,

f is the frequency of fine sediment layers with gas entry pressures ΔP_c (Equation 3), where frequency is defined as the number of fine layers per unit distance in the flow direction, and

the other parameters are as defined earlier.

If $\nabla P = f?P_c$, capillary sealing prevents the flow of both fluid phases. If $\nabla P = f?P_c$, viscous forces control the rate of flow and flow is linearly related to pressure gradients in excess of $f?P_c$.

The experiments described show that the flow domain described by (Equation 7a) is easy to establish in grain-size layered media. Capillary barriers prevent flow when (Equation 7a) pertains. The pressure jump at each fine layer and the temperature dependence of this jump are well described by the capillary equation (Equation 3). Blockage in the experiments occurs when the pore space is occupied about half by gas and half by water. The experiments show that the blockage offered by each fine layer is independent, and that the blockage of all layers must be exceeded for flow through the system to occur. This independence survives the forced passage of up to 12 pore volumes of two-phase fluid through the fine-layer seal. This resiliency and the magnitude of the capillary pressure drops, which we anticipate are about the same magnitude in basins as in our experiments, suggests capillarity could be an important mechanism for reducing permeability and controlling flow in sedimentary basins.

Acknowledgments

We thank The Gas Research Insititute for funding the work reported in this paper (Grant #5093-260-2689 to L. Cathles) and Don Turcotte for useful discussions and suggestions.

References

Bear, J., 1972, Dynamics of Fluids in Porous Media: American Elsevier Publishing Company, New York, 764 p.

Behar, E., R. Simonet, and E. Rauzy, 1985, A new non-cubic equation of state: Fluid Phase Equilibria, v. 21, p. 237–255.

Behar, E., R. Simonet, and E. Rauzy, 1986, Erratum: Fluid Phase Equilibria, v. 31, p. 319.

Berg, R.R., 1975, Capillary pressures in stratigraphic traps, AAPG Bull., v. 59, n. 6, p. 939–956.

Borresen, K. A., and A., Graue, 1997, Fluid flow across capillary heterogeneities, experiments and simulations: Transport in Porous Media, v. 29, p.141–158.

Cathles, L. M., 2001, Capillary seals as a cause of pressure compartmentation in sedimentary basins: GCSSEPM Foundation 21st Bob F. Perkins Research Conference, this issue.

Celia, M. A., P. C. Reeves, and L. A. Ferrand, 1995, Recent advances in pore scale models for multiphase flow in porous media: Reviews of Geophysics, Supplement, p. 1049–1057.

Chaouche, M., N. Rakotomalala, D. Salin, B. Xu, and Y. C. Yortsos, 1994, Capillary effects in drainage in heterogeneous porous media: Continuum modeling, experiments, and pore network simulations: Chemical Engineering Science, v. 49, no. 15, p. 2447–2466.

Freeze, R. A., and J. A. Cherry, 1979, Groundwater: Prentice-Hall, Englewood Cliffs, NJ, 604 p.

Graton, L. C., and H. J. Fraser, 1935, Systematic packing of spheres with particular relation to porosity and permeability: Jour. Geology, v. 63, p. 785–909.

Huang, Y., P. S. Ringrose, and K. S. Sorbie, 1995, Capillary trapping mechanisms in water-wet laminated rocks: SPE Reservoir Engineering, November, p. 287–292.

Kung, K.-J. S., 1990, Preferential flow in a sandy vadose zone: 1. Field Observation: Geoderma, v. 46, p. 51–58.

Kung, K.-J. S., 1990, Preferential flow in a sandy vadose zone: 2. Mechanisms and Implications: Geoderma, v. 46, p. 59–71.

Lenormand, R., E. Touboul, and C. Zarcone, 1988, Numerical models and experiments on immicible displacements in porous media: Jour. Fluid Mechanics, v. 189, p. 165–187.

Matthews, C. S., and D. G. Russell, 1967, Pressure buildup and flow tests in wells: Henry H. Doherty Series Monograph Volume 1, Society of Petroleum Engineers, New York, 167p.

Miyazaki, T., 1988, Water flow in unsaturated soil in layered slopes: Jour. Hydrology, v. 102, p. 201–214.

Revil, A., P. A. Pezard, and M. Darot, 1997, Electrical conductivity, spontaneous potential and ionic diffusion in porous media, in M. A. Lovell, M. A., and Harvey, P. K., Developments in Developments in Petrophysics: Geological Society Special Publications 122, p. 253–275.

Revil, A., and L. M. Cathles, 1999, Permeability of shaly sands: Water Resources Research, v. 35, no. 3, p. 651–662.

Ross, B., 1990, The diversion capacity of capillary barriers: Water Resources Research, v. 26, no. 10, p. 2625–2629.

Schowalter, T.T., 1979, Mechanics of secondary hydrocarbon migration and Entrapment: AAPG Bull., v. 63, no. 5, p. 723–760.

Sen, P.N., C. Scala, and M. H. Cohen, 1998, Self-similar model for sedimentary rocks with application to the dielectric constant of fused glass beads, Geophysical Research Letters, v. 25, p. 691–694.

Steenhuis, T.S., K.-J. S. Kung, J.-Y. Parlange, J. S. Selker, and X.-X. Chen, 1990, Flow regimes in sandy soils with inclined layers: Tenth Annual American Geophysical Union Hydrology Days, Colorado State University, Fort Collins.

Steenhuis, T., and J.-Y. Parlange, 1991, Comment on the diversion capacity of capillary barriers, Water Resources Research, v. 27, no. 8, p. 2155–2156.

Stumm, W., and Morgan, J. J., 1996, Aquatic Chemistry: John Wiley, New York, 1022 p.

Van Duijn, C. J., J. Molenaar, and M. J. De Neef, 1995, The effect of capillary forces on immiscible two-phase flow in heterogeneous porous media: Transport in Porous Media, v. 21, p. 71–93.

Washburn, E. W., West, C. J., and Dorsey, N. E., eds., 1928, International critical tables of numerical data, physics, chemistry, and technology: National Research Council of USA, McGraw Hill, New York.